DOI: 10.1002/ejic.201100154

The First *P*-Stereogenic 1D Coordination Polymers with the Metal Centers in the Backbone

Christine Salomon,[a,b] Daniel Fortin,[a] Naïma Khiri,[b] Sylvain Jugé,*[b] and Pierre D. Harvey*[a]

Keywords: Silver / Copper / Phosphane ligands / Chirality / Coordination polymers

The enantiomeric ligands (*R*,*R*)- and (*S*,*S*)-bis(*o*-anisylphenylphosphanyl)methane (*R*,*R*-**22** and *S*,*S*-**22**) and (*R*,*R*)- and (*S*,*S*)-bis(phenyl-*m*-xylylphosphanyl)methane (*R*,*R*-**23** and *S*,*S*-**23**; dppm*), were treated with $[Cu(NCCH_3)_4](BF_4)$ and $AgBF_4$ to produce the binuclear complexes $[Cu_2(dppm^*)_2(NCCH_3)_4](BF_4)_2$ or $[Ag_2(dppm^*)_2](BF_4)_2$, respectively. Then, these complexes were used as building blocks to prepare the first *P*-chirogenic 1D coordination polymers $\{[M_2(dppm^*)_2(dmb)_2](BF_4)_2\}_n$ [dppm* = (*R*,*R*)-**22**, (*S*,*S*)-**22**, (*R*,*R*)-**23**, (*S*,*S*)-**23**, M = Cu, Ag, dmb = 1,8-diisocyano-*p*-menthane] where M is part of the backbone of the polymer chain. The isostructural nature of these new polymers with the achiral parent polymers, $\{[M_2(dppm)_2(dmb)_2](BF_4)_2\}_n$ (M = Cu, Ag), was unambiguously demonstrated with a combination of methods including ^1H NMR, chemical analysis, UV/Vis spectrometry, emission spectroscopy and emission lifetime measurements. The structure of the bimetallic complex $[Ag_2(R,R\text{-}\mathbf{23})_2](BF_4)_2$ was solved by X-ray crystallography, and all enantiomeric complexes and polymers were characterized by circular dichroism spectroscopy.

Introduction

Design of coordination polymers and crystal engineering using diphosphane assembling ligands is a topic of current interest.[1,2] The most common diphosphane bridging ligands are those of the type $Ph_2P(CH_2)_mPPh_2$ with m = 1–6. The smallest of the series is bis(diphenylphosphanyl)-methane (dppm), but one can also associate the structurally related bis(diphenylarsanyl)methane (dpam) and bis(dimethylphosphanyl)methane (dmpm). In the early days, coordination polymers were obtained by bridging binuclear complexes of the 4th and 5th row transition elements by dppm or dmpm such as polymers **1**–**3** (Scheme 1).[3,4]

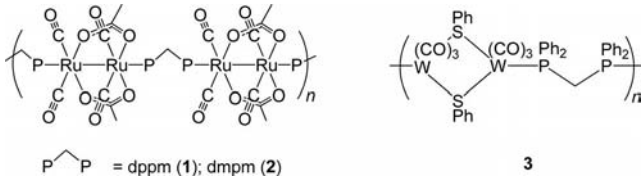

Scheme 1.

[a] Département de Chimie, Université de Sherbrooke, Sherbrooke, PQ, Canada, J1K 2R1
Fax: +1-819-821-8017,
E-mail: Pierre.Harvey@USherbrooke.ca
[b] Institut de Chimie Moléculaire de l'Université de Bourgogne (ICMUB), UMR CNRS 5260, Université de Bourgogne, 9 avenue Alain Savary, B. P. 47870, 21078 Dijon Cedex, France
Fax: +33-3-80396113
E-mail: sylvain.juge@u-bourgogne.fr

Since these early reports, the field has been totally dominated by coordination polymers based on copper(I) and silver(I).[5–9] The resulting 1D polymers are invariably built upon mixed bridging ligands (i.e. dppm or dmpm and an assembling ligand) and there is often only a single bridging ligand keeping the polymer chain together (see **4**,[5] **5**,[6] **6**,[6] **7**,[7] **8**–**10**,[8] **11**, **12**,[9] **13**–**16**,[10] and **17**;[11] Scheme 2).

On some occasions, however, 1D polymers could also be built upon multi-bridging strategies such as those illustrated in Scheme 3 (see polymers **18**,[12] **19**,[13] **20**, and **21**[14]). They exhibit two general structures, ladder (**18**) and rigid rods (**19**–**21**), and consequently they are symmetric objects.

To the best of our knowledge, no chiral-dppm or *P*-chirogenic coordination polymer with the metal atoms in the backbone has been reported. There is one example of a *P*-chirogenic polymer, polymer **25** (Scheme 4), that falls into this category but the metal fragment, $PtCl_2$, is not part of the backbone.[15] The diphosphane binap [2,2′-bis(diphenylphosphanyl)-1,1′-binaphthyl] has also been used to produce chiral coordination polymeric materials but in such cases the P atom is not chirogenic as it is in this case.[16]

Recently, the enantiomeric ligands (*R*,*R*)- and (*S*,*S*)-bis(*o*-anisylphenylphosphanyl)methane [dppm*; (*R*,*R*)-**22**, (*S*,*S*)-**22**; Scheme 5] were used to prepare the C_3-symmetry $[Pd_3(dppm^*)_3(CO)(O_2CCF_3)](CF_3CO_2)$ clusters which were characterized by X-ray crystallography and circular dichroism spectroscopy.[17]

We now wish to report the first *P*-chirogenic 1D (and rigid rod) coordination polymers $\{[M_2(dppm^*)_2(dmb)_2]$-

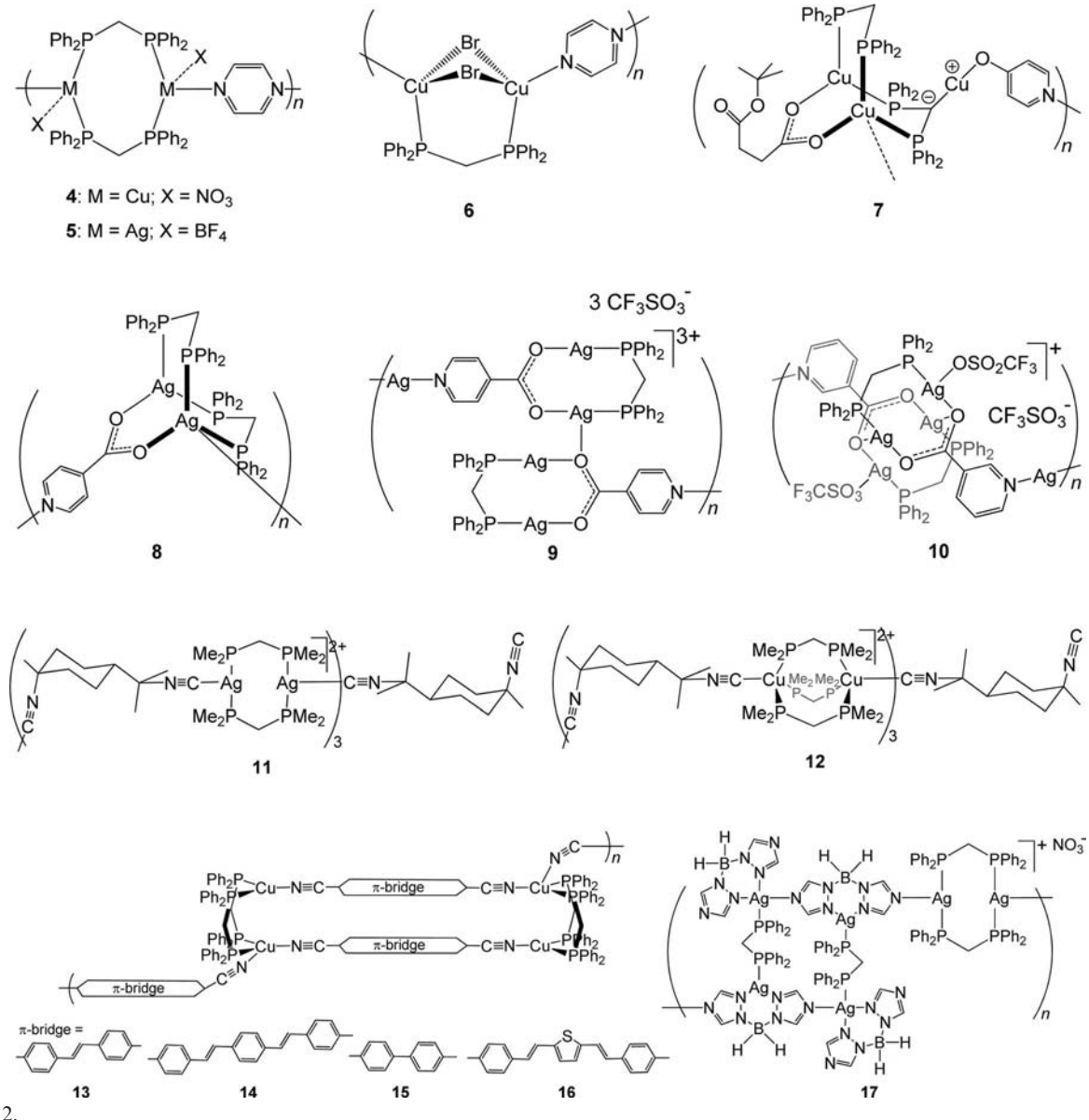

Scheme 2.

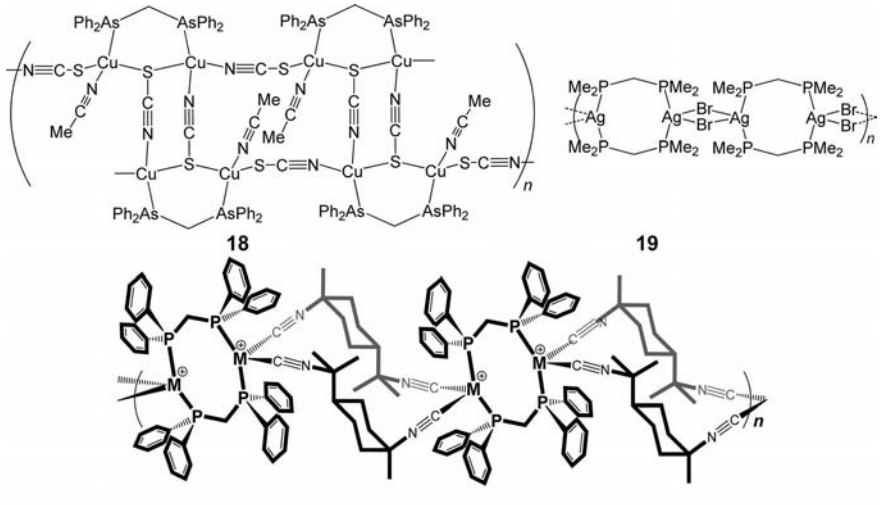

([M2(dppm)2(dmb)2](BF4)2)n, dmb = 1,8-diisocyano-*p*-menthane: **20** (M = Cu), **21** (M = Ag)

Scheme 3.

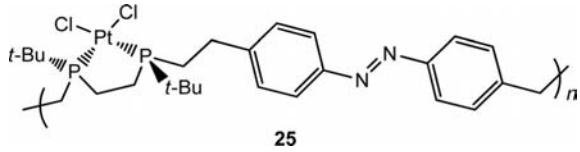

25

Scheme 4.

$(BF_4)_2\}_n$ [dppm* = (*R*,*R*)-**22**, (*S*,*S*)-**22**, (*R*,*R*)-**23**, (*S*,*S*)-**23** (Scheme 5), M = Cu, Ag, dmb = 1,8-diisocyano-*p*-menthane] where M is part of the polymer backbone. In the absence of X-ray structure determination, ^{1}H NMR, chemical analysis, UV/Vis spectrometry, emission spectroscopy, and photophysical measurements were used to unambiguously demonstrate the isostructural nature of these new polymers with the parent dppm-containing polymers **20** and **21**.[14]

Results and Discussion

Syntheses and characterization. The stereoselective syntheses of the (*R*,*R*)- and the (*S*,*S*)-ligands **22** were performed in several steps using the (+)- or (–)-ephedrine methodology, via formation of the chlorophosphane–borane intermediate **26**.[18] The key step of the synthesis is the methano bridge formation from the reaction of the carbanion derived from the methylphosphane–borane **27** with the chlorophosphane–borane **26**; see Scheme 6, only the (*R*,*R*)-version is shown.[18]

Thus, the reaction of the (*S*)-*o*-anisylchlorophenylphosphane–borane **26** with the MeLi reagent affords the corresponding (*R*)-methylphosphane–borane **27** with inversion of configuration at the P-centre. After deprotonation of the methylphosphane–borane **27** with *n*BuLi, reaction with the (*S*)-chlorophosphane–borane **26** afforded the protected (*R*,*R*)-diphosphane–diborane **28** in good yields. The enantiomeric purity was checked by chiral HPLC using racemic samples of **28**. The desired free dppm* ligand **22** was obtained cleanly after decomplexation of the diborane complex **28** with DABCO (Scheme 6).

The chiral coordination polymers were synthesized in two steps. First, the binuclear complexes $[Cu_2(dppm^*)_2(NCCH_3)_4](BF_4)_2$ {from dppm* + $Cu(BF_4)_2$ + Cu in CH_3CN}[19a] or $[Ag_2(dppm^*)_2](BF_4)_2$ (from dppm* + $AgBF_4$ in CH_3CN)[19b] {dppm* = (*R*,*R*)-**22**, (*S*,*S*)-**22**, (*R*,*R*)-**23**, (*S*,*S*)-**23**} were prepared in the same manner as the parent achiral dppm complexes using the *P*-chirogenic dppm* ligands, with isolated yields ranging from 50–98% (Scheme 7). Thus, four new *P*-chirogenic (binuclear) complexes in both enantiomeric forms were prepared and characterized.

In the $[Ag_2\{(R,R)\text{-}\mathbf{23}\}_2](BF_4)_2$ case, the X-ray crystal structure was obtained (Figure 1). As expected, this complex exhibits two (*R*,*R*)-**23** ligands bridging two Ag^I metals, forming an eight-membered ring in a "boat" conformation. The Ag atoms are separated by 2.932(1) Å, a distance typical of complexes containing the $Ag_2(P\text{^}P)_2^{2+}$ frame with no formal Ag–Ag bond.[20,21] The global C_2-symmetry of the complex is also evident. Full details of the structure are provided in the Supporting Information. The ^{31}P NMR spectra of the bimetallic $[Ag_2(dppm^*)_2](BF_4)_2$ complexes exhibit a doublet of apparent triplets, due to the $^1J_{AgP}$ coupling between phosphorus and the combination of the silver isotopes ^{107}Ag and ^{109}Ag, in 48 and 52% natural abundance, respectively (Table 1).[22] Conversely, the $[Cu_2(dppm^*)_2(NCCH_3)_4](BF_4)_2$ species are characterized by a singlet consistent with the absence of direct ^1J coupling (Table 2).

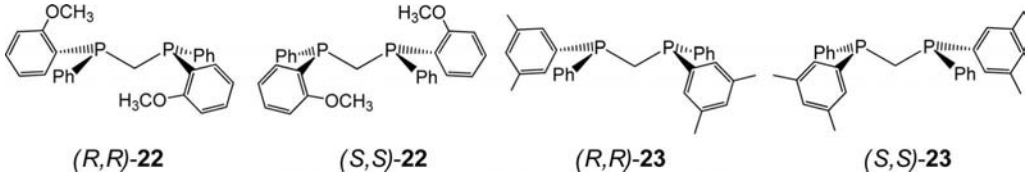

Scheme 5.

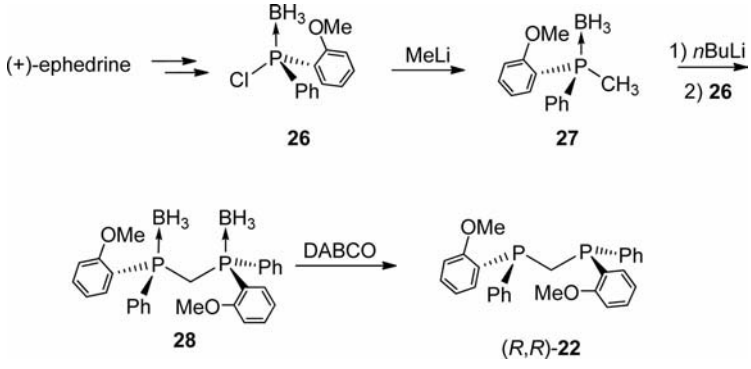

Scheme 6.

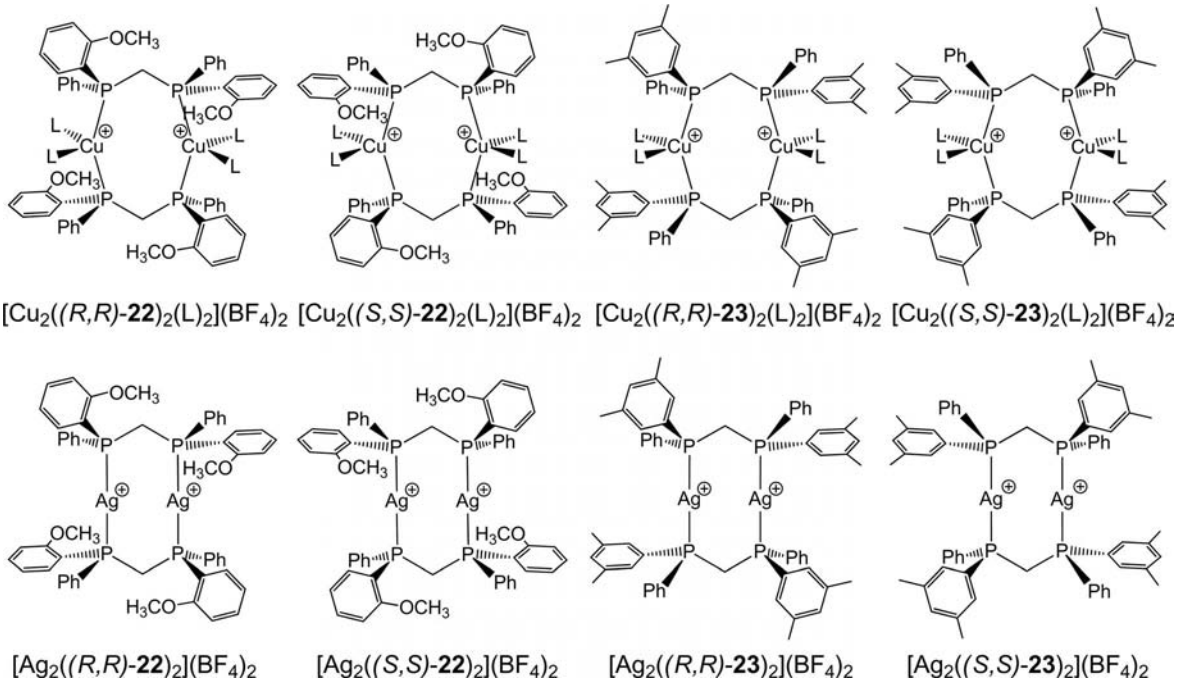

Scheme 7. L = CH_3CN; BF_4^- anions not shown.

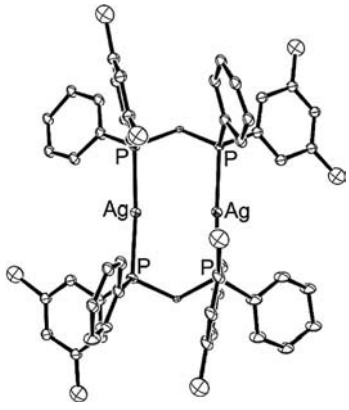

Figure 1. ORTEP representation $[Ag_2\{(R,R)\text{-}\mathbf{23}\}_2](BF_4)_2$. The ellipsoids are shown with 50% probability. The H-atoms and counter anions are not shown for clarity.

The corresponding *P*-chirogenic coordination polymers were prepared by reacting the enantiomeric *P*-chirogenic binuclear complexes with 2 equiv. of the assembling diisocyanide ligand dmb. The general reactions are shown in Equations (1) and (2), with dppm* = (*R*,*R*)-**22**, (*S*,*S*)-**22**, (*R*,*R*)-**23**, and (*S*,*S*)-**23**.

$$[Cu_2(dppm^*)_2(NCCH_3)_4](BF_4)_2 + 2\ dmb \rightarrow \{[Cu_2(dppm^*)_2(dmb)_2](BF_4)_2\}_n + 4\ CH_3CN \quad (1)$$

$$[Ag_2(dppm^*)_2](BF_4)_2 + 2\ dmb \rightarrow \{[Ag_2(dppm^*)_2(dmb)_2](BF_4)_2\}_n \quad (2)$$

The coordination of dmb is evidenced by the change in $\nu(N{\equiv}C)$ going from the uncoordinated dmb ligand (at $2135 \pm 5\ cm^{-1}$) to the coordination polymers (at $2180 \pm 5\ cm^{-1}$). Both ^1H NMR and chemical analyses agree with the stoichiometry of the polymers. The isolated yields are compared in Table 1 and all appear good to excellent except for one case [($\{Ag_2\{(R,R)\text{-}\mathbf{23}\}_2(dmb)_2\}(BF_4)_2$), 24%]. No attempt was made to increase the yield as there was enough material to carry out the characterization.

Table 1. ^{31}P NMR spectroscopic data for Ag_2 complexes and their coordinating polymers with dmb.

Entry		δ[a,c]	$^1J_{107Ag-P}$[b]	$^1J_{109Ag-P}$[b]	$\lvert{}^1J_{Ag-P} + {}^3J_{Ag-P}\rvert$[b]
1	(*R*,*R*)-**22**	–31.2	–	–	–
2	(*R*,*R*)-**23**	–33.5[d]	–	–	–
3	$[Ag_2\{(R,R)\text{-}\mathbf{22}\}_2](BF_4)_2$	+2.2	487	561	525
4	$[Ag_2\{(R,R)\text{-}\mathbf{23}\}_2](BF_4)_2$	+8.5	471	543	508
5	$\{[Ag_2\{(R,R)\text{-}\mathbf{22}\}_2(dmb)_2](BF_4)_2\}_n$	+0.2	–	–	425
6	$\{[Ag_2\{(R,R)\text{-}\mathbf{23}\}_2(dmb)_2](BF_4)_2\}_n$	+3.6	375	429	402

[a] δ in ppm relative to H_3PO_4. [b] In Hz. [c] CD_3CN at 295 K. [d] $CDCl_3$ at 295 K.

Table 2. ^{31}P NMR spectroscopic data for Cu_2 complexes and their coordinating polymers with dmb.

Entry		δ[a,b]
1	(*R*,*R*)-**22**	–31.2
2	(*R*,*R*)-**23**	–33.5[c]
7	$[Cu_2\{(R,R)\text{-}\mathbf{22}\}_2(NCCH_3)_4](BF_4)_2$	–16.9
8	$[Cu_2\{(R,R)\text{-}\mathbf{23}\}_2(NCCH_3)_4](BF_4)_2$	–10.9
9	$\{[Cu_2\{(R,R)\text{-}\mathbf{22}\}_2(dmb)_2](BF_4)_2\}_n$	–20.7
10	$\{[Cu_2\{(R,R)\text{-}\mathbf{23}\}_2(dmb)_2](BF_4)_2\}_n$	–7.6

[a] δ in ppm relative to H_3PO_4. [b] CD_3CN at 295 K. [c] $CDCl_3$ at 295 K.

Attempts to obtain crystals suitable for X-ray crystal structure determinations stubbornly failed. In order to demonstrate the isostructurality of the polymers with the parent dppm-containing polymers **20** and **21** (Scheme 3), UV/Vis and luminescence spectroscopy were used and, more importantly, emission lifetime measurements were also performed. The argument is that if the chromophore $[M(CNR)_2(P)_2]$ is the same for all cases, the position of the emission bands should be the same. In addition, if the emission lifetimes are also in the same neighbourhood, then the overall structure must be the same for both the dppm- and dppm*-containing polymers. This point will be discussed further below. Moreover, the use of the absorption data alone is not ideal since these features appear below 400 nm and many overlapping bands appear in this same spectral range (200–400 nm).

Circular dichroism. In order to demonstrate that the target four *P*-chirogenic binuclear complexes (Scheme 5) and the four *P*-chirogenic polymers in both enantiomeric forms were obtained, circular dichroism spectroscopy (CD) was used. The typical UV/Vis spectra of a ligand [(*R*,*R*)-**22** for example] and its corresponding binuclear complex and coordination polymer are shown in Figure 2. The ligand absorbs in the 200–310 nm range (typical for π,π*-type transitions for substituted benzenes), whereas the binuclear complex and coordination polymer absorb in the 200–380 nm window. These absorptions indicate a region where CD activity is expected. Indeed, the CD spectra for the ligands exhibit positive and negative signals for both enantiomeric forms precisely in this same spectral window (see Figure 3 as an example).

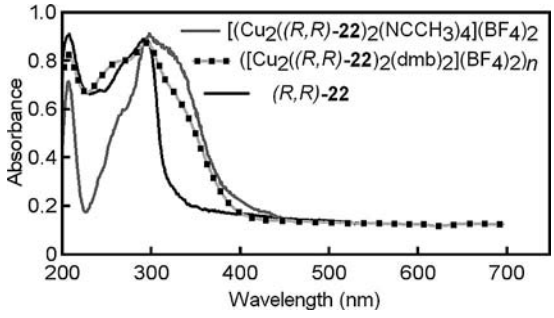

Figure 2. Examples of solid state UV/Vis spectra of the ligand (*R*,*R*)-**22**, the binuclear complex $[Cu_2\{(R,R)\text{-}\mathbf{22}\}_2](BF_4)_2$ and coordination polymer $\{[Cu_2\{(R,R)\text{-}\mathbf{22}\}_2(dmb)_2](BF_4)_2\}_n$ at 298 K.

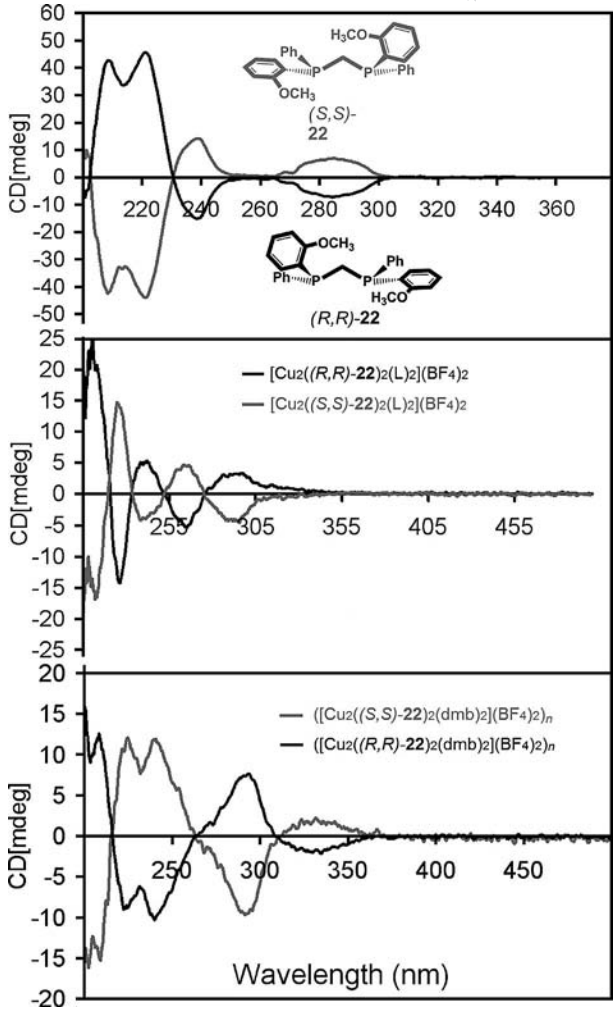

Figure 3. Comparison of the CD of the ligands (*R*,*R*)-**22**, (*S*,*S*)-**22**, the corresponding binuclear complexes, $[Cu_2(dppm^*)_2](BF_4)_2$ and coordination polymers $\{[Cu_2(dppm^*)_2(dmb)_2](BF_4)_2\}_n$ [dppm* = (*R*,*R*)-**22**, (*S*,*S*)-**22**] as typical examples; solvent: acetonitrile.

The appearance of a new red shifted bands in both the UV/Vis and CD spectra in the 320–360 nm region going from the uncoordinated ligand to the binuclear complexes and coordination polymers is common and fully consistent with new spin-allowed electronic transitions involving the metallic center appearing on the low energy side of the spectra. Indeed, these were previously theoretically addressed for polymers of the type $[M(dmb)_2^+]_n$ (M = Cu, Ag) and $Cu_2(dppm)_2(O_2CCH_3)^+$.[23,24] These bands are expectedly assigned to metal-to-ligand-charge-transfer (MLCT) for the d^{10} electronic configurations for Cu^I and Ag^I.

The CD data for the binuclear complexes and polymers are listed in Table 3. Again, the CD spectra of both enantiomeric forms of the binuclear complexes and coordination polymers exhibit the expected mirror-image relationship. A slight red shift of the low-energy (positive and negative) signals for the binuclear complexes and coordination polymers in comparison with that of the corresponding ligands is also observed following the same trend that is observed in the UV/Vis spectra.

Table 3. CD data for the $[Cu_2(dppm^*)_2(CH_3CN)_4](BF_4)_2$ and $[Ag_2(dppm^*)_2](BF_4)_2$, binuclear complexes, and the $\{[M_2(dppm^*)_2(dmb)_2](BF_4)_2\}_n$, polymers in acetonitrile at 298 K.

Binuclear complex	(*R*,*R*)			(*S*,*S*)		
	λ_{max} [nm]	θ [mdeg][a]	θ [deg cm^2 dmol^{-1}][b]	λ_{max} [nm]	θ [mdeg][a]	θ [deg cm^2 dmol^{-1}][b]
dppm* = **22**	210	25.2	190000	212	–16.8	–127000
M = Cu	226	–14.2	–107000	225	14.7	110000
	238	5.1	38200	238	–4.2	–31200
	265	–5.3	–39900	263	4.6	34800
	294	3.3	24500	296	–4.5	–34000
	212	–18.3	–137000	213	18.7	126000
	228	3.2	23500	226	–6.5	–43700
dppm* = **23**	248	1.3	9500	249	–1.7	–11400
M = Cu	254	1.5	11200	258	–1.3	–8700
	284	–0.9	–6900	285	1.1	7100
	201	49.9	319000	206	–47.1	–335000
dppm* = **22**	224	–19.0	–122000	224	13.5	95500
M = Ag	259	–2.0	–12900	253	2.6	18400
	276	14.7	93900	278	–15.4	–110000
	297	–7.1	–45200	301	6.4	45500
dppm* = **23**	207	–45.1	–319000	209	45.3	262000
M = Ag	249	1.2	8300	248	–0.7	–5100
	272	1.4	10000	273	–1.3	–9400
	281	2.1	14600	280	–1.7	–12300
	288	1.8	12500	289	–1.5	–10800
Polymer	(*R*,*R*)			(*S*,*S*)		
	λ_{max} [nm]	θ [mdeg][a]	θ [deg cm^2 dmol^{-1}][b]	λ_{max} [nm]	θ [mdeg][a]	θ [deg cm^2 dmol^{-1}][b]
dppm* = **22**	208	12.5	82000	209	–15.3	–120000
M = Cu	222	–10.0	–65300	225	12.1	94800
	240	–10.3	–67300	241	11.9	93400
	294	7.6	49900	292	–9.7	–76000
	335	–2.2	–14200	332	2.2	17600
dppm* = **23**	210	–18.3	–119000	208	18.3	119000
M = Cu	226	3.1	20200	228	–4.0	–25900
	246	1.0	6400	245	–1.4	–8900
	278	1.2	7600	278	–1.0	–6400
dppm* = **22**	207	26.2	181000	208	–32.0	–220000
M = Ag	225	–1.2	–8400	224	3.5	23900
	234	6.2	42900	235	–5.4	–37100
	256	–5.1	–35100	254	5.0	34900
	278	14.2	97800	276	–13.3	–92100
dppm* = **23**	213	–25.2	–174000	212	21.1	145000
M = Ag	241	2.0	13900	239	–1.7	–11700
	258	–1.2	–8200	259	1.0	7100
	271	2.4	16400	273	–2.3	–15600
	298	–1.5	–10500	297	1.1	7800

Uncertainties: (a) ±0.5 mdeg. (b) θ: $(\theta_{exp.} \times M/c \times l \times 10) \pm 100$ deg cm^2 dmol^{-1} with M: molar mass (g mol^{-1}), c: concentration (g mL^{-1}), l: optical path length, 0.2 cm.

One of the concerns in coordination polymers is that in the solid state these polymers could be real polymers but in solution these could break down in very small oligomers including even a monomer. Our group spent a large amount of time investigating mono-ligand and mixed-ligand coordination polymers, namely for isocyanides and phosphanes, and demonstrating clearly the presence of oligomer (solution) and polymer (solid state) equilibrium. The most striking example is the $\{[Ag(dmb)_2]^+\}_n$ polymer which is 7–9 units long in acetonitrile solution (Scheme 8).[25]

But also show an obvious equilibrium between the U-shaped and Z-shaped coordinated dmb ligand (Scheme 9) as crystallographically demonstrated in Equation (3).[26]

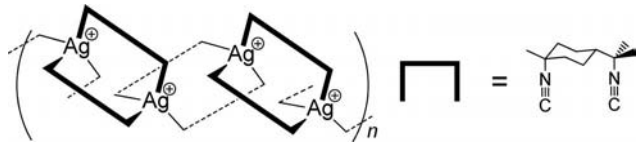

Scheme 8.

$$\{[Ag(U\text{-}dmb)_2]^+\}_n \leftrightarrow \{[Ag(U\text{-}dmb)(Z\text{-}dmb)]^+\}_n \leftrightarrow \{[Ag(U\text{-}dmb)_2]^+\}_n \quad (3)$$

This finding shows that the isocyanine systems are indeed dynamic and exists as oligomers in solution. However, they return to polymers when these oligomers return to the

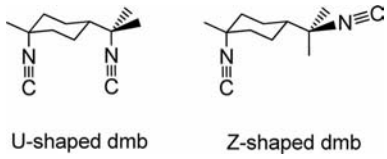

Scheme 9.

solid state. Moreover, in the mixed-ligand diphosphane-dmb polymers (Scheme 10) exhibit oligomers lengths varying from 7 to 16, somewhat similar to the polymers presented in Schemes 7 and 8).[27]

The fact that the lowest energy CD signals of the ligands and the oligomers (dimers and oligomers) are different meaning that the oligomers are not very small (simple di-

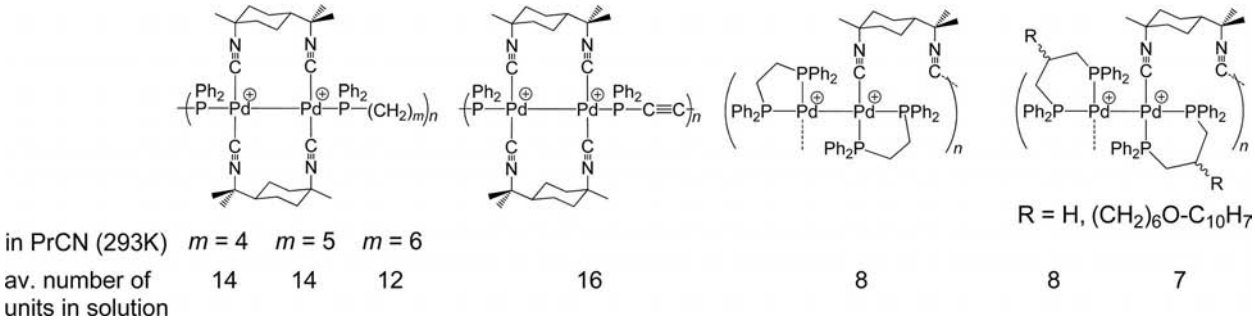

Scheme 10.

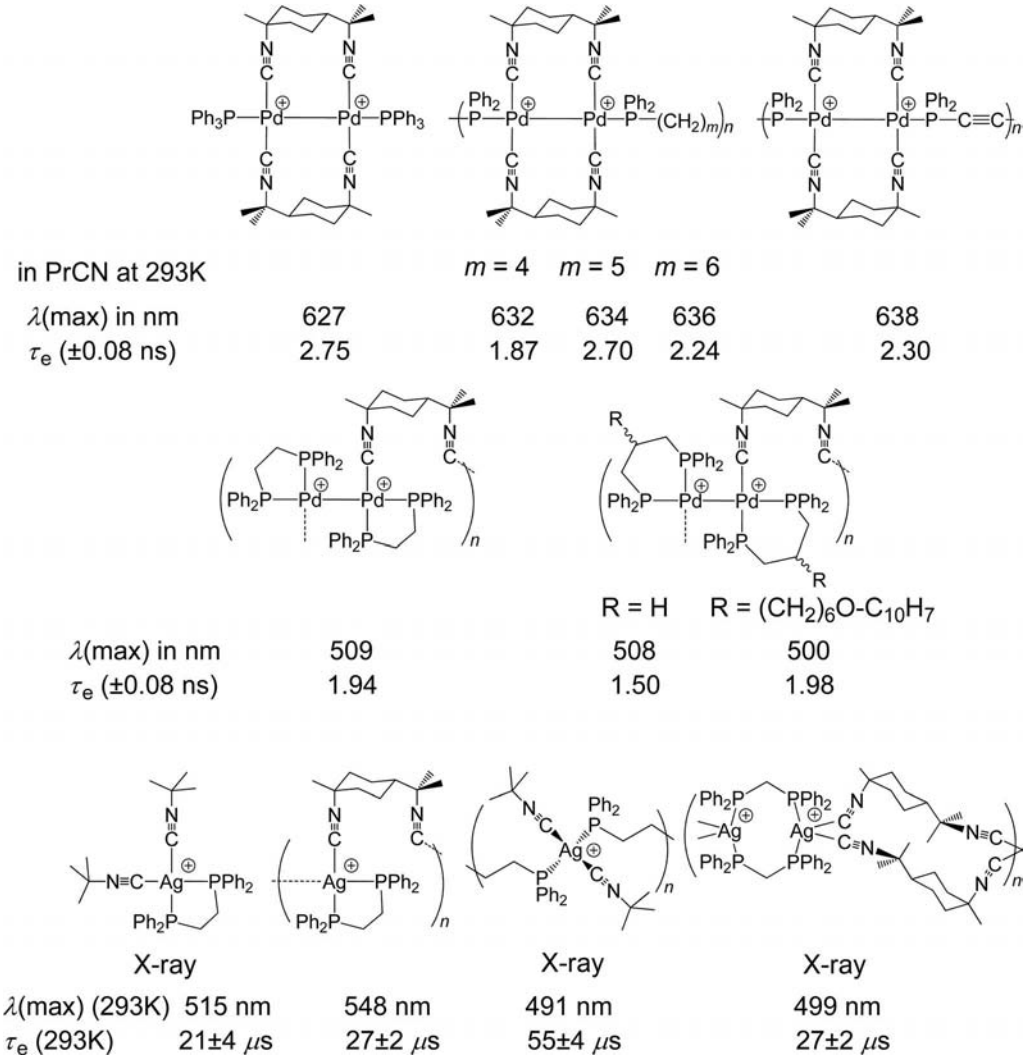

Scheme 11.

mers, trimers or tetramers) but are somewhat longer and retain the dmb in the coordination sphere. All in all, four *P*-chirogenic binuclear complexes and the four *P*-chirogenic polymers in both enantiomeric forms have been prepared and characterized by CD spectroscopy.

Luminescence Spectroscopy. As stated above, in the absence of X-ray diffraction data for the coordination polymers, luminescence spectroscopy and measurement of emission lifetimes (τ_e) were used to confirm the isostructural 1-D nature of these new materials. Prior to doing so, literature precedents are necessary to explain the method. Scheme 11 compares the emission maxima and lifetime of several examples of mixed-ligand d^9-d^9 Pd_2-bonded species and d^{10} Ag^I species, both monomers and oligomers where the ligands are dmb, *tert*-butyl isocyanide and diphosphanes.[14,27,28]

The d^9-d^9 Pd_2-bonded species, both monomeric and oligomeric species are characterized by lowest energy singlet and triplet dσ→dσ* energy excited states. This series can be separated into two categories, chelating diphosphanes [such as bis(diphenylphosphanyl)ethane (dppe) and -propane (dppp)][28] and bridging diphosphanes [such as bis-(diphenylphosphanyl)butane (dppb), -pentane (dpppent), -hexane (dpph), and -ethynylene]. The former series in PrCN at 77 K exhibits emission maxima between 500 and 510 nm and an emission lifetime between 1.50 and 1.98 μs (average 1.80 μs).[27] The latter series exhibits emission maxima ranging from 627 to 638 nm, and lifetimes from 1.87 to 2.75 averaging 2.37 μs.[28] This comparison indicates a clear relationship between the structure (*cis* vs. *trans*) and the photophysical data. The replacement of an axial bridging diphosphane ligand by two monodentate PPh_3 axial ligands does not drastically change the position and lifetime of the emission band. The Ag^I species can also be separated into two categories as well, chelate and bridging diphosphanes. The mononuclear complex $[Ag(dppe)(CN\textit{t}Bu)]^+$ and polymer $\{Ag(dppe)(dmb)^+\}_n$ in the solid state at 298 K exhibit MLCT excited state with similar emission maxima at 515 and 548 nm and similar emission lifetimes of 21 and 27 μs, respectively.[28] This means that the replacement of dmb by two CN*t*Bu ligands does change drastically the electronic and steric effect on the excited state properties and the local structure. This observation corroborates that seen for the replacement of an axial diphosphane ligand by two axial monodentate PPh_3 groups as stated above. The 1D $\{Ag(dpppen)(CN\textit{t}Bu)_2^+\}_n$ and $\{Ag_2(dppm)_2(dmb)_2^{2+}\}_n$ (**21**)[14] coordination polymers in the solid state at 298 K exhibit emission maxima at 491 and 499 nm, with lifetimes of 55 and 27 μs, respectively. Although there is no change in emission maxima, due to the good similarity in chemical environment, the emission lifetime changes by a factor of 2. This change reflects the change in polymer structure ···Ag(diphos)Ag(diphos)··· vs. ···$Ag(diphos)_2$Ag-(dmb)···. Similarly, the $\{Cu(dpppen)(CN\textit{t}Bu)_2^+\}_n$ and $\{Cu_2(dppm)_2(dmb)_2^{2+}\}_n$ (**20**) exhibit emission lifetime of 42 and 24 μs, respectively.[14]

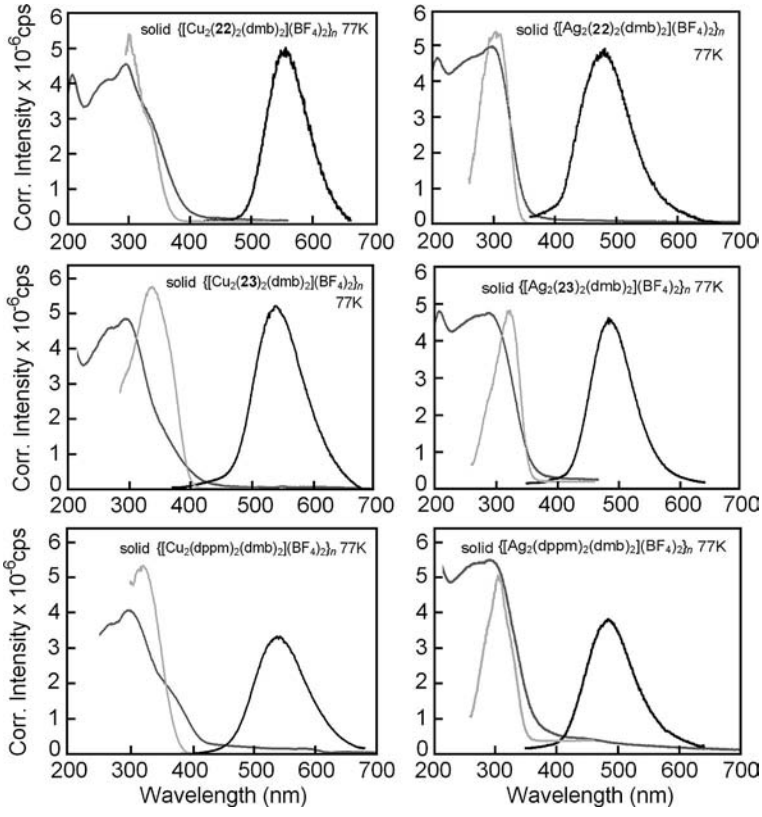

Figure 4. Absorption (in butyronitrile solution at 298 K; dark grey), excitation (light grey) and emission spectra (black) of the chiral and achiral $\{[Cu_2(dppm^*)_2(dmb)_2](BF_4)_2\}_n$ polymers (dppm* = dppm, **22**, **23**) in the solid state at 77 K.

Both binuclear complexes and polymers are strongly luminescent at 77 K (Figure 4). In this work, the $[M(CNR)_2(P)_2]$ chromophore environment can also be confirmed from the comparison of the emission maxima between the structurally known $\{[M_2(dppm)_2(dmb)_2](BF_4)_2\}_n$ polymers (M = Cu, Ag) and the corresponding chiral $\{[Cu_2(dppm^*)_2(dmb)_2](BF_4)_2\}_n$ ones (dppm* = **22**, **23**; see Figure 4 and Table 4).

Table 4. UV/Vis and luminescence data (solid state) of the binuclear complexes and polymers.

	λ_{em} [nm] 77K[a]	τ_e 77K[b]
$\{[Cu_2(\mathbf{22})_2(dmb)_2](BF_4)_2\}_n$	550	435 ± 15 μs
$\{[Cu_2(\mathbf{23})_2(dmb)_2](BF_4)_2\}_n$	536	450 ± 25 μs
$\{[Cu_2(dppm)_2(dmb)_2](BF_4)_2\}_n$	543	380 ± 10 μs
$\{[Ag_2(\mathbf{22})_2(dmb)_2](BF_4)_2\}_n$	479	210 ± 10 μs
$\{[Ag_2(\mathbf{23})_2(dmb)_2](BF_4)_2\}_n$	480	265 ± 15 μs
$\{[Ag_2(dppm)_2(dmb)_2](BF_4)_2\}_n$	481	260 ± 10 μs
$[Cu_2(\mathbf{22})_2(NCCH_3)_4](BF_4)_2$	482	117 ± 20 ns
$[Cu_2(\mathbf{23})_2(NCCH_3)_4](BF_4)_2$	492	73.5 ± 1.6 ns
$[Cu_2(dppm)_2(NCCH_3)_4](BF_4)_2$	488	152 ± 10 ns
$[Ag_2(\mathbf{22})_2](BF_4)_2$	440	34.3 ± 0.5 ns
$[Ag_2(\mathbf{23})_2](BF_4)_2$	449	36.1 ± 1.6 ns
$[Ag_2(dppm)_2](BF_4)_2$	447	40.3 ± 5 ns

[a] In butyronitrile. [b] λ_{ex} = 391 nm; $\lambda_{exp.t}$ = 550 nm for all the polymers, $\lambda_{exp.}$ = 490 nm for all three $[Cu_2(dppm^*)_2(NCCH_3)_4](BF_4)_2$ complexes, and = 450 nm for all three $[Ag_2(dppm^*)_2](BF_4)_2$ species.

The 1D nature can be confirmed from the similarity in τ_e values based on the fact that the amplitude of the radiative (k_e) and non-radiative (k_{nr}) rate constants [$\tau_e = 1/(k_e + k_{nr})$] are properties dependent upon the molecular structures (molecular symmetry and relative frequencies of the Franck–Condon active vibrations). In this way, we can distinguish between known 1D $\{[M_2(dppm)_2(dmb)_2](BF_4)_2\}_n$ polymers (M = Cu, Ag) and any other network (i.e. 2D and 3D).

At 77 K, the λ_{em} values (Table 3) vary with $\{[Cu_2(dppm^*)_2(dmb)_2](BF_4)_2\}_n$ (536–550 nm) > $\{[Ag_2(dppm^*)_2(dmb)_2](BF_4)_2\}_n$ (479–481 nm) ≥ $[Cu_2(dppm)_2(NCCH_3)_4](BF_4)_2$ (482–492 nm) > $[Ag_2(dppm)_2](BF_4)_2$ (440–449 nm) where dppm* is dppm, **22** or **23**. On one hand, these values confirm the similarity in λ_{em} maxima within the same series of dppm* ligand, confirming the similarity in the $[M(CNR)_2(P)_2]$ chromophore, but also allow for differentiation between Cu and Ag species and between polymers and dimers.

Similarly, the τ_e values (Table 3) vary as $\{[Cu_2(dppm^*)_2(dmb)_2](BF_4)_2\}_n$ (380–450 μs) > $\{[Ag_2(dppm^*)_2(dmb)_2](BF_4)_2\}_n$ (210–265 μs) > $[Cu_2(dppm)_2(NCCH_3)_4](BF_4)_2$ (0.07–0.15 μs) > $[Ag_2(dppm)_2](BF_4)_2$ (0.03–0.04 μs) where dppm* is dppm, **22** or **23**. The similarity in τ_e within the series confirms the structure about the $[M(CNR)_2(P)_2]$ chromophores as being 1D. Moreover, the fact that the τ_e values for the Cu-containing species are shorter than those for the Ag ones, reflects upon the heavy atom effect which is a consequence of the strong spin-orbit coupling of the heavier silver atom. The fact that the τ_e values for the polymers are larger than those for the binuclear complexes reflects upon the larger rigidity of the tetrahedral $[M(CNR)_2(P)_2]$ chromophore locked inside the 1D polymer structure in comparison with those of the binuclear complexes $[Cu_2(dppm)_2(NCCH_3)_4](BF_4)_2$ and $[Ag_2(dppm)_2](BF_4)_2$ where looser Cu–$NCCH_3$ and $Ag^+\cdots F–BF_3^-$ interactions takes place.

In order to corroborate the similarity in 1D structure of the $\{[Ag_2(dppm^*)_2(dmb)_2](BF_4)_2\}_n$ polymers and **20**, we also have examined the steric environment about the *ortho*- and *meta*-positions of the dppm ligand in the parent achiral polymer (Figure 5). While the *meta*-positions are clear from obstruction, some of the *ortho*-positions are less so. Indeed, there are a total of eight possible *ortho*-positions per repetitive unit where OMe groups can be placed. Of these eight, two are simply cluttered (labelled with #), and two others sterically difficult (labelled with §) but available. The four other *ortho*-positions are fully accessible. Hence, the formation of the polymers $\{[Cu_2(dppm^*)_2(dmb)_2](BF_4)_2\}_n$ and $\{[Ag_2(dppm^*)_2(dmb)_2](BF_4)_2\}_n$ [dppm* = (*R*,*R*)-**22**, (*S*,*S*)-**22**, (*R*,*R*)-**23**, and (*S*,*S*)-**23**] are corroborated from a simple modeling stand point.

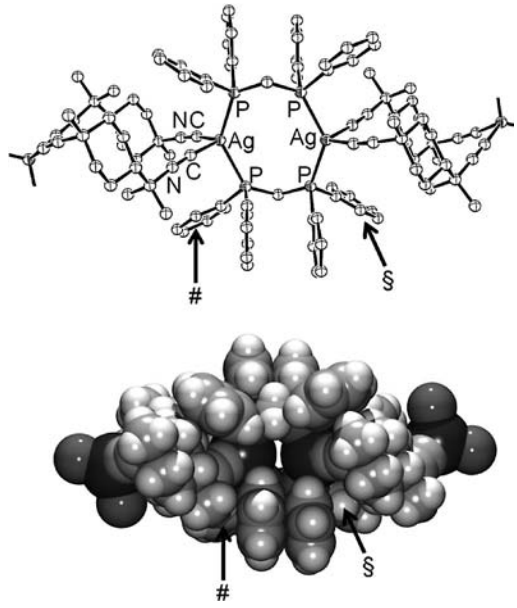

Figure 5. Bottom: space filling representation of a segment of the achiral $\{[Ag_2(dppm)_2(dmb)_2](BF_4)_2\}_n$ polymer stressing the two *ortho*-positions, # [note the C_i symmetry of the $Ag_2(dppm)_2$ unit], that are too sterically demanding to insert a substitutant such as OCH_3. The outside atoms are dummy atoms for drawing purposes. Top; ball and stick model, bottom, space filling model.

Thermal stability. During the course of this study, the thermal stability of the new polymers was tested by thermal gravimetric analysis (TGA; Figure 6). The materials are stable up to about 190 °C, consistent with what is known about the decomposition of the M-dmb unit based on recent studies on $\{[M(diphos)(dmb)]BF_4\}_n$ and $\{[Pd_2(diphos)_2(dmb)](ClO_4)_2\}_n$ coordination polymers [M = Cu, Ag; diphos = $Ph_2P(CH_2)_mPPh_2$, m = 2, 3],[28] $\{[M_2(dppm)_2(dmb)_2](BF_4)_2\}_n$ (M = Cu, Ag),[14] and $\{[M_2(dppm)_2(dmb)](BF_4)_2\}_n$ (M = Pd, Pt).[29] The second major thermal event occurs between 260 and 450 °C and is most likely due to

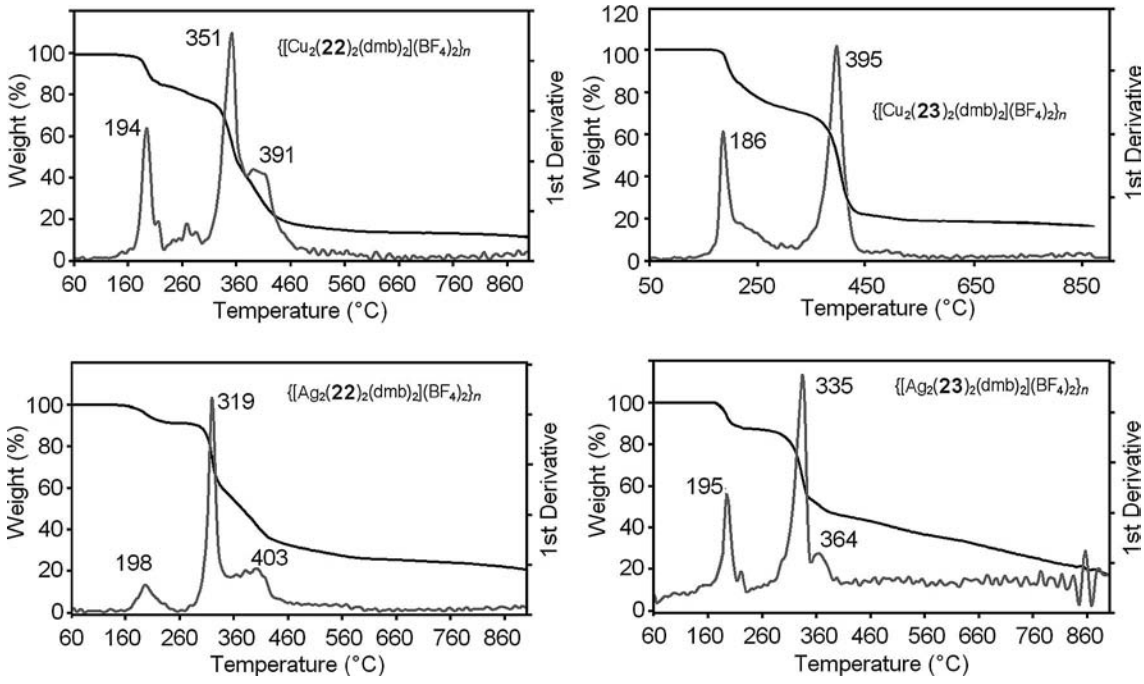

Figure 6. TGA traces for the $\{[M_2(dppm^*)_2(dmb)_2](BF_4)_2\}_n$ polymers.

decomposition of the dppm* ligand mixed with the loss of the BF_4^- anions. All in all, these new materials exhibit a very strong resemblance with thermal behavior observed for the aforementioned polymers.

Conclusions

The first *P*-chirogenic 1D coordination polymers in both enantiomeric forms were prepared and characterized by circular dichroism spectroscopy among other techniques. These are of the type $\{[M_2(dppm^*)_2(dmb)_2](BF_4)_2\}_n$ where dppm* is one of the chiral ligands (*R*,*R*)-**22**, (*S*,*S*)-**22**, (*R*,*R*)-**23**, and (*S*,*S*)-**23**, and M is either Cu or Ag. The isostrutural nature of these new polymers with the parent symmetric dppm-containing polymers, $\{[M_2(dppm)_2(dmb)_2](BF_4)_2\}_n$, was unambiguously demonstrated with a combination of methods including ^{1}H NMR, chemical analysis, UV/Vis spectrometry, and measurements of the emission lifetimes in the solid state in comparison with the corresponding achiral analogues for which a crystal structure is known in which M = Ag.[14] The concept of slight structure modification of the dppm ligand presented in this work opens the door to new material design in coordination and organometallic chemistry. For example, the commercial diphosphane $Ph_2P(CH_2)_mPPh_2$ ligands (m = 2–9) are well known for making coordination polymers.[1,2] Corresponding chiral versions of ligands similar to those presented in this work should lead to new crystal motifs and optical properties.

Experimental Section

Materials: The 1,8-diisocyano-*p*-menthane (dmb) was prepared according to a published procedure[30] in which the bridging ligands (*R*,*R*)- or (*S*,*S*)-bis(*o*-anisylphenylphosphanyl)methane and (*R*,*R*)- or (*S*,*S*)-bis(*m*-xylylphenylphosphanyl)methane were substituted for dppm. The (*R*,*R*)-ligands were prepared via their corresponding diborane complexes by reaction of the α-carbanion derived from the (*Rp*)-(–)-*N*-methyl-[(1*R*,2*S*)(2-hydroxy-1-phenyl)ethyl]amino-*o*-anisylphenylphosphane–borane or (*Rp*)-(–)-*N*-methyl-[(1*R*,2*S*)(2-hydroxy-1-phenyl)ethyl]aminoxylylphenylphosphane–borane with the (*S*)-*o*-anisylchlorophenylphosphane–borane or (*S*)-*o*-xylylchlorophenylphosphane, respectively, employing a modified methodology starting from the (+)-ephedrine.[18] The (*S*,*S*)-ligands were prepared in a similar way starting from (–)-ephedrine. The chiral phosphane–boranes **26** were also prepared by methods described in the literature.[18] The detailed synthesis of the anisyl derivatives are described below. To avoid repetition, only the (*R*,*R*)-series are described. The synthesis of the corresponding xylyl-containing materials is reported elsewhere.[31]

(R_P)-(–)-*o*-Anisylmethylphenylphosphane–Borane (27): In a 50 mL two-necked flask equipped with a magnetic stirrer, 2 mmol of the (R_P)-(–)-*N*-methyl-[(1*R*,2*S*)-(2-hydroxy-1-phenyl)ethyl]amino-*o*-anisylphenylphosphane–borane was introduced via an argon inlet and rubber septum. A solution of HCl in toluene (0.38 M, 11.0 mL, 4.2 mmol, 2.1 equiv.) was next added whilst stirring at room temperature, without previous dissolution of (R_P)-(–)-*N*-methyl-[(1*R*,2*S*)-(2-hydroxy-1-phenyl)ethyl]amino-*o*-anisylphenylphosphane–borane. After 1 h, the precipitate of ephedrine hydrochloride was filtered off using a Millipore 4 μm filter, and the excess HCl was removed using several vacuum/argon cycles. The toluene solution of chlorophosphane–borane **26** obtained was used without further purification. The solution containing **26** was cooled to –78 °C and MeLi (0.87 M, 5.7 mL, 5 mmol, 2.5 equiv.) was added. The reaction mixture was warmed to room temp. over a period of 1 h, and then hydrolysed with water. The organic phase was removed and the aqueous layer was extracted with CH_2Cl_2. The combined extracts were dried with $MgSO_4$, then concentrated. The residue was purified by chromatography on a short column of silica gel using a 7:3 by volume mixture of toluene/petroleum ether to

give the phosphane–borane **27**. It was recrystallized from a mixture of isopropyl alcohol/*n*-hexane, affording enantiomerically pure phosphane–borane as white needle crystals. Enantiomeric excess was determined by HPLC [Chiralcel OK, *n*-hexane/*i*PrOH (80:20), 1 mL/min, λ = 254 nm, $t_R(R)$ = 11.1 min, $t_R(S)$ = 21.4 min]; yield 90%; white crystals; m.p. 76–77 °C. $[\alpha]_D^{25}$ = –25.8 (c = 1.3, CH_3OH) for *ee* > 99%; R_f = 0.55 (toluene). IR (KBr): $\tilde{\nu}$ = 3060 (C–H), 3000–2840 (C–H), 2380 (B–H), 1590, 1580, 1480, 1460, 1430, 1280, 1250, 1180, 1135, 1110, 1060, 1020 cm^{-1}. ^1H NMR ($CDCl_3$): δ = 0.40–1.50 (q, $^3J_{BH}$ = 88 Hz, 3 H, BH_3), 1.94 (d, $^2J_{PH}$ = 10.6 Hz, 3 H, P–CH_3), 3.67 (s, 3 H, OCH_3), 6.88 (dd, J = 8.3, J = 3.4 Hz, 1 H, H_{arom} *o*An), 7.05 (t, J = 7.4 Hz, 1 H, H_{arom} *o*An), 7.33–7.56 (m, 4 H, H_{arom}), 7.56–7.69 (m, 2 H, H_{arom}) ppm. ^{11}B NMR{^1H}($CDCl_3$): δ = –37.1 (d) $^1J_{PB}$ = 62.6 Hz. $^{13}C\{^1H\}$ NMR ($CDCl_3$): δ = 10.7 (d, $^1J_{PC}$ = 42.3 Hz, P-*C*H_3), 55.4 (O*C*H_3), 129.1 (d, J_{PC} = 11.0 Hz, C_{arom}), 111.6 (d, J_{PC} = 4.9 Hz, C_{arom}), 119.3 (d, J_{PC} = 62.6 Hz, C_{arom}), 120.8 (d, J_{PC} = 10.9 Hz, C_{arom}), 128.1 (d, J_{PC} = 10.9 Hz, C_{arom}), 131.1 (d, J_{PC} = 11.6 Hz, C_{arom}), 131.3 (d, J_{PC} = 2.4 Hz, C_{arom}), 132.0 (d, J_{PC} = 66.1 Hz, C_{arom}), 133.9 (d, J_{PC} = 11.2 Hz, C_{arom}), 134.1 (d, J_{PC} = 1.7 Hz, C_{arom}) ppm. ^{31}P NMR{^1H} ($CDCl_3$): δ = +9.2 (q, $^1J_{PB}$ = 66.1 Hz) ppm. MS (EI) *m*/*z* (%) 230 (M^+ – BH_3, 100), 119 (43), 183 (35), 91 (57). $C_{14}H_{18}BOP$ (244.0769): calcd. C 68.89, H 7.43; found C 68.96, H 7.59.

(*R*,*R*)-Bis(*o*-anisylphenylphosphanyl)methane–Borane (28): A 100 mL two-necked flask equipped with a magnetic stirrer, an argon inlet and a rubber septum was charged with 1.08 g of the phosphane–borane **27** (4.40 mmol, 3 equiv.) in 10 mL of THF. The solution was cooled to 0 °C and 2.8 mL of *n*BuLi (1.6 M in *n*-hexane, 4.40 mmol, 3 equiv.) was added dropwise. The reaction was maintained at this temperature for 30 min, after which the cooling bath was removed and the reaction stirred at room temperature for 90 min. After cooling to –78 °C, a freshly prepared toluene solution of the chlorophosphane–borane **26** (1.47 mmol, 1 equiv.) was added dropwise with stirring to the anion solution. The mixture was slowly allowed to increase to room temperature overnight. After hydrolysis, the aqueous layer was extracted with 3 × 30 mL of CH_2Cl_2, and the combined extracts were dried with $MgSO_4$, then concentrated. The residue was purified by chromatography on a short column of silica gel with toluene as solvent, to give the diphosphane–diborane complex. It was recrystallized from CH_2Cl_2, by slow diffusion of heptane, affording diastereomerically and enantiomerically pure white needle crystals; yield 80%; m.p. 187 °C; R_f = 0.33 (toluene). $[\alpha]_D^{20}$ = +45 (c = 0.5, $CHCl_3$) for 99% *ee*. IR (solid): $\tilde{\nu}$ = 3019–2942, 2408, 1589, 1479, 1458, 1435, 1152, 1277, 1152, 1061, 1017 cm^{-1}. ^1H NMR ($CDCl_3$): δ = 0.2 (m, $^1J_{BH}$ = 116 Hz, 6 H, BH_3), 3.53 (s, 6 H, OCH_3), 3.54 (2d, $^2J_{HH}$ = 13.9, $^2J_{PH}$ = 11.6 Hz, 2 H, CH_2), 6.65 (dd, $^3J_{HH}$ = 8.3, $^4J_{PH}$ = 2.9 Hz, 2 H, Ar), 6.83 (t, $^3J_{HH}$ = 7.5 Hz, 2 H, Ar), 7.09–7.21 (m, 6 H, Ar), 7.28–7.37 (m, 6 H, Ar), 7.53–7.64 (dd, $^3J_{HH}$ = 7.6, $^3J_{PH}$ = 14.8 Hz, 2 H, Ar) ppm. ^{11}B NMR {^1H}($CDCl_3$): δ = [ppm] –37.6 (br. s). ^{13}C NMR ($CDCl_3$): δ = [ppm] 18.5 (t, J_{PC} = 28 Hz, *C*H_2), 55.2 (O*C*H_3), 111.0 (d, J_{PC} = 4 Hz, C_{arom}), 114.0 (d, J_{PC} = 54 Hz, C_q), 121.0 (d, J_{PC} = 14 Hz, C_{arom}), 128.3 (d, J_{PC} = 10 Hz, C_{arom}), 130.2 (d, J_{PC} = 2 Hz, C_{arom}), 130.6 (d, J_{PC} = 10 Hz, C_{arom}), 132.5 (d, $^1J_{PC}$ = 60 Hz, C_q), 134.5 (d, J_{PC} = 2 Hz, C_{arom}), 137.3 (d, J_{PC} = 18 Hz, C_{arom}),162.0 (d, J_{PC} = 3 Hz, C_{arom}), $^{31}P\{^1H\}$ NMR ($CDCl_3$): δ = +13.5 (m, $^1J_{PB}$ = 34 Hz) ppm. HRESI-MS (CH_2Cl_2) calcd. for $C_{27}H_{32}B_2NaO_2P_2$ [M + Na^+]: 495.1961; found: 495.1956. Anal. calcd. (%) for $C_{27}H_{32}B_2O_2P_2$, 0.9CH_2Cl_2: C 60.70, H 6.17; found: C 60.96, H 6.30. The diastereomeric and enantiomeric excess was controlled by HPLC analysis on a Chiralpak AD Daicel column, eluent: *n*-hexane/*i*PrOH (9:1), 1 mL/min, λ = 254 nm; (*R*,*R*), t_R = 52 min; (*S*,*S*)-enantiomer t_R = 9 min; (*R*,*S*), t_R = 26 min.

(*R*,*R*)-(–)-Bis(*o*-anisylphenylphosphanyl)methane (22): The diphosphane–diborane **28** (0.11 mmol) was placed in a three-necked flask fitted with a reflux condenser, a magnetic stirrer, and an argon inlet. A solution of DABCO (0.44 mmol) in toluene (4 mL) was added, and the flask was purged three times with argon. The mixture was heated to 50 °C for 12 h and the crude product was rapidly filtered off on a neutral alumina column (15 cm height, 2 cm diameter) using a degassed toluene/AcOEt (9:1) mixture as solvent. After removal of the solvent, the free ligand **22** was obtained quantitatively and used without further purification. R_f = 0.45 (toluene; CCM silica gel, flash chromatography on neutral alumina). $[\alpha]_D^{20}$ = –48 (c = 0.5, $CHCl_3$) for 99% *ee*. ^1H NMR ($CDCl_3$): δ = 2.82 (s, 2 H, CH_2), 3.64 (s, 6 H, OCH_3), 6.70 (d, J = 8.19 Hz, 2 H, Ar), 6.79 (t, J = 7.24 Hz, 2 H, Ar), 6.97–7.04 (m, 2 H, Ar), 7.08–7.23 (m, 2 H, Ar), 7.24–7.29 (m, 6 H, Ar), 7.47–7.55 (m, 4 H, Ar) ppm. $^{13}C\{^1H\}$ NMR ($CDCl_3$): δ = 22.2 (t, J_{PC} = 22 Hz, *C*H_2), 54.3 (O*C*H_3), 109.1 (s, C_{arom}), 119.7 (s, C_{arom}), 126.9 (t, J_{PC} = 4 Hz, C_q), 127.1 (t, J_{PC} = 4 Hz, C_{arom}), 127.4 (s, C_{arom}), 128.9 (s, C_{arom}), 131.5 (t, J_{PC} = 4 Hz, C_{arom}), 132.4 (t, J_{PC} = 11 Hz, C_{arom}), 136.3 (t, J_{PC} = 4.5 Hz, C_q),159.8 (t, J_{PC} = 6.5 Hz, C_q) ppm. $^{31}P\{^1H\}$ NMR ($CDCl_3$): δ = –30.6 ppm. HRESI-MS (CH_2Cl_2) calcd. for $C_{27}H_{27}O_2P_2$ [M^+]: 445.1481; found: 445.1497.

[Cu_2(dppm*)$_2$($NCCH_3$)$_4$](BF_4)$_2$ (dppm* = 22 and 23) Complexes: To a flask equipped with a magnetic stirrer and an argon inlet, 0.207 mmol (49.1 mg) of anhydrous $Cu(BF_4)_2$ and 5 mL of acetonitrile distilled were introduced. Approximately 50 mg of powdered metallic copper was added. The mixture was stirred for 1.5 h with exclusion of light. To a second flask equipped with a magnetic stirrer and an argon inlet, 0.207 mmol of *P*-chirogenic diphosphane **22** or **23** and 10 mL of distilled acetonitrile were introduced. The first solution was transferred to the second flask using a cannula and the mixture was stirred overnight. After filtration, the volume of the filtrate was reduced under reduced pressure, and [Cu_2(**22**)$_2$-(CH_3CN)$_4$](BF_4)$_2$ or [Cu_2(**22**)$_2$(CH_3CN)$_4$](BF_4)$_2$, respectively, was precipitated by adding diethyl ether.

[Cu_2(22**)$_2$($NCCH_3$)$_4$](BF_4)$_2$:** Yield 92% (0.1291 g), white solid, m.p. 226 °C. $[\alpha]_D^{20}$ = –8.2 (c = 0.09, $CHCl_3$). IR (solid): $\tilde{\nu}$ = 2279, 1634, 1582, 1481, 1432, 1275, 1245, 1058 cm^{-1}. ^1H NMR (CD_3CN): δ = 7.73 (br., 4 H, Ar), 7.38 (m, 4 H, Ar), 7.21 (m, 4 H, Ar), 7.10 (br., 20 H, Ar), 6.45 (br., 4 H, Ar), 3.41 (m, 4 H, CH_2), 3.14 (s, 12 H, OCH_3), 1.98 (s, 12 H, CH_3CN) ppm. $^{13}C\{^1H\}$ NMR ($CDCl_3$): δ = 139.5 (C_{arom}), 139.2 (C_{arom}), 138.7 (C_{arom}), 138.0 (C_{arom}), 136.5 (C_{arom}), 135.0 (C_{arom}), 133.5 (C_{arom}), 126.0 (C_{arom}), 122.7 (CH_3CN), 116.8 (C_{arom}), 110.0 (C_{arom}), 60.0 (O*C*H_3), 27.1 (*C*H_2), 2.89–5.06 (CN*C*H_3) ppm. $^{31}P\{^1H\}$ NMR ($CDCl_3$): δ = –10.3 (s) ppm. $C_{62}H_{64}B_2Cu_2F_8N_4O_4P_4$ (1353.80): calcd. C 54.95, H 4.73, O 4.73, N 4.14; found C 55.23, H 4.89, O 4.54, N 3.85. HRESI-MS (CH_2Cl_2); found 507.0756 (z = 2) for Cu_2(**22**)$_2$, calcd. 507.0699.

[Cu_2(23**)$_2$($NCCH_3$)$_4$](BF_4)$_2$:** Yield 87% (0.1267 g), white solid, m.p. 92 °C, $[\alpha]_D^{20}$ = –6 (c = 0.05, $CHCl_3$). IR (solid): $\tilde{\nu}$ = 2316, 2271, 1632, 1597, 1440, 1054 cm^{-1}. ^1H NMR (CD_3CN): δ = 7.26 (br., 12 H, Ar), 7.16 (m, 8 H, Ar), 6.89 (br., 12 H, Ar), 3.42 (m, 4 H, CH2), 2.12 (s, 24 H, CH_3), 1.97 (s, 12 H, CH_3CN) ppm. $^{13}C\{^1H\}$ NMR ($CDCl_3$): δ = 143.97 (C_{arom}), 143.74 (C_{arom}), 139.29 (C_{arom}), 137.5 (C_{arom}), 137.0 (C_{arom}), 135.7 (C_{arom}), 135.1 (C_{arom}), 133.7 (C_{arom}), 122.7 (*C*NCH_3), 40.4 (*C*H_2), 25.62 (*C*H_3), 6.12–5.07 (CN*C*H_3) ppm. $^{31}P\{^1H\}$ NMR ($CDCl_3$): δ = –5.54 (s) ppm. $C_{66}H_{72}B_2Cu_2F_8N_4P_4$ (1345.91): calcd. C 58.84, H 5.35, N 4.16; found C 59.11, H 5.52, N 3.96. HRESI-MS (CH_2Cl_2); found 1041.1927 (z = 1) for Cu_2(**23**)$_2$Cl, calcd. 1041.1921.

$[Ag_2(dppm^*)_2](BF_4)_2$ complexes (dppm* = 22 and 23) Complexes: A 25 mL two necked flask equipped with a magnetic stirrer, an argon inlet, and a rubber septum was charged with **22** or **23** (43.6 mg, 0.098 mmol) and $Ag(BF_4)$ (19 mg, 0.098 mmol) in distilled acetonitrile (5 mL). The mixture was stirred overnight with exclusion of light. After evaporation of the solvent, the product was precipitated with a mixture CH_2Cl_2/n-hexane.

$[Ag_2(\mathbf{22})_2](BF_4)_2$: Yield 66% (41.6 mg), white solid, m.p. 186 °C (dec.), $[\alpha]_D^{20}$ = –22 (*c* = 0.51, $CHCl_3$). IR (solid): $\tilde{\nu}$ = 1627, 1571, 1586, 1473, 1432, 1274, 1249, 1058, 743 cm^{-1}. ^1H NMR (CD_3CN): δ = 7.46 (br., 2 H, Ar), 7.41 (br., 8 H, Ar), 7.28 (br., 10 H, Ar), 7.90 (br., 6 H, Ar), 6.80 (br., 8 H, Ar), 6.56 (br., 2 H, Ar), 3.77 (m, 4 H, CH_2), 3.48 (s, 12 H, OCH_3) ppm. $^{13}C\{^1H\}$ NMR ($CDCl_3$): δ = 139.5 (C_{arom}), 138.9 (C_{arom}),137.7 (C_{arom}), 137.5 (C_{arom}), 136.9 (C_{arom}), 135.9 (C_{arom}), 133.8 (C_{arom}), 133.6 (C_{arom}), 126.3 (C_{arom}), 110.0 (C_{arom}), 60.4 (O*C*H$_3$), 27.3 (*C*H$_2$) ppm. $^{31}P\{^1H\}$ NMR (CD_3CN): δ = –1.78 and –1.94 (dd, $^1J_{Ag-P}$ = 522, $^2J_{P,P}$ = 19 Hz) ppm. $C_{54}H_{52}B_2Cu_2F_8O_4P_4$ (1189.59): calcd. C 50.70, H 4.07; found C 50.80, H 4.27. HRESI-MS (ACN/MeOH); found 551.0482 (z = 2) for $Ag_2(\mathbf{22})_2$, calcd. 551.0454.

$[Ag_2(\mathbf{23})_2](BF_4)_2$: Yield 95% (70.5 mg), white solid, m.p. 248 °C. IR (solid): $\tilde{\nu}$ = 1601, 1582, 1488, 1488, 1440, 1058 cm^{-1}. ^1H NMR (CD_3CN): δ = 7.30 (br., 12 H, Ar), 7.01 (m, 18 H, Ar), 6.85 (br., 2 H, Ar), 3.58 (m, 4 H, CH_2), 2.06 (s, 24 H, CH_3) ppm. $^{13}C\{^1H\}$ NMR ($CDCl_3$): δ = 144.3 (C_{arom}), 138.2 (C_{arom}), 137.7 (C_{arom}), 136.5 (C_{arom}), 135.2 (C_{arom}), 135.0 (C_{arom}), 134.2 (C_{arom}),110.1 (C_{arom}), 27.7 (*C*H$_2$), 25.5 (*C*H$_3$) ppm. $^{31}P\{^1H\}$ NMR ($CDCl_3$): δ = 7.22 and 7.08 (dd, $^1J_{Ag-P}$ = 508, $^2J_{P,P}$ = 18 Hz) ppm. $C_{58}H_{60}Ag_2B_2F_8P_4{\cdot}(CH_3CH_2)_2O$ (1270.35): calcd. C 55.38, H 5.21; found C 55.22, H 5.08. HRESI-MS (ACN/MeOH); found 547.0885 (z = 2) for $Ag_2(\mathbf{23})_2$, calcd. 547.0868.

$\{[Cu_2(dppm^*)_2(dmb)_2](BF_4)_2\}_n$ (dppm* = 22 and 23) Polymers: These polymers were synthesized starting from $[Cu_2(\mathbf{22})_2(CH_3CN)_4](BF_4)_2$ $[Cu_2(\mathbf{23})_2(CH_3CN)_4](BF_4)_2$ according to a procedure described for the achiral polymer $\{[Cu_2(dppm)_2(dmb)_2](BF_4)_2\}_n$.[14]

Specifically, $[Cu_2(\mathbf{22})_2(CH_3CN)_4](BF_4)_2$ (0.1056 g, 0.078 mmol) was dissolved in 14 mL of distilled acetonitrile. A 29.6 mg (0.156 mmol) amount of dmb was dissolved separately in a round flask containing 25 mL of distilled acetonitrile. This latter colorless solution was slowly added dropwise to the former. The mixture was stirred for 2 h prior to being reduced to 7.5 mL in vacuo. A 75 mL volume of diethyl ether was added to the reaction mixture precipitating the white product, which was filtered off and dried in vacuo.

$\{[Cu_2(\mathbf{22})_2(dmb)_2](BF_4)_2\}_n$: Yield 73% (89 mg), m.p. 146 °C. $[\alpha]_D^{20}$ = –14 (*c* = 0.24, $CHCl_3$). IR (solid): $\tilde{\nu}$ = 2185, 1585, 1470, 1436, 1275, 1245, 1058 cm^{-1}. ^1H NMR (CD_3CN): δ = 7.86 (br., 3 H, Ar), 7.49 (br., 1 H, Ar), 7.32 (m, 3 H, Ar), 7.16 (m, 6 H, Ar), 7.10 (m, 3 H, Ar), 7.02 (br., 15 H, Ar), 6.74 (br., 1 H, Ar), 6.36 (br., 4 H, Ar), 3.49 (m, 4 H, CH_2), 3.25 (s, 12 H, OCH_3), 2.15–1.50 (m, 36 H, dmb) ppm. $^{13}C\{^1H\}$ NMR ($CDCl_3$): δ = 142.9 (CN), 141.1 (C_{arom}), 138.0–135.1 (br. m, C_{arom}), 133.5 (C_{arom}) 125.9 (br., C_{arom}), 116.9 (C_{arom}), 66.1 (C_q), 60.7 (C_q), 60.3 (O*C*H$_3$), 46.3 (*C*H), 40.8 (*C*H$_2$), 31.6 (*C*H$_2$), 27.5 (*C*H$_3$), 27.2 (P*C*H$_2$P), 26.4 (CH_3) ppm. $^{31}P\{^1H\}$ NMR ($CDCl_3$): δ = –2.1 (br), –9.3 (br), –13.69 (br) ppm. $(C_{39}H_{44}BCuF_4N_2O_2P_2)_n$: calcd. C 59.62, H 5.61, O 4.08, N 3.57; found C 59.47, H 5.44, O 4.19, N 3.34.

$\{[Cu_2(\mathbf{23})_2(dmb)_2](BF_4)_2\}_n$: Yield 67% (82 mg), m.p. 172 °C. $[\alpha]_D^{20}$ = –3.5 (*c* = 0.19, $CHCl_3$). IR (solid): $\tilde{\nu}$ = 2178, 1627, 1451, 1476, 1316, 1174, 1095, 1062 cm^{-1}. ^1H NMR (CD_3CN): δ = 7.24 (br., 12 H, Ar), 7.12 (br., 10 H, Ar), 6.87 (br., 10 H, Ar), 3.28 (br., 4 H, CH_2), 2.12 (s, 24 H, CH_3), 1.47 (br., 36 H, dmb) ppm. $^{13}C\{^1H\}$ NMR ($CDCl_3$): δ = 143.7 (CN), 139.4 (C_{arom}), 137.5 (br., C_{arom}), 135.9 (C_{arom}), 135.0 (C_{arom}), 134.4 (C_{arom}), 133.6 (C_{arom}), 110.1 (C_{arom}), 48.7 (C_q),41.5 (*C*H), 33.1 (*C*H$_2$), 31.5 (*C*H$_3$), 27.6 (P*C*H$_2$P), 25.7 (*C*H$_3$) ppm. $^{31}P\{^1H\}$ NMR ($CDCl_3$): δ = –2.2 (s) ppm. $(C_{41}H_{48}BCuF_4N_2P_2)_n$: calcd. C 63.0, H 6.15, N 3.59; found C 63.13, H 5.87, N 3.81.

$\{[Ag_2(dppm^*)_2(dmb)_2](BF_4)_2\}_n$ (dppm* = 22 and 23) Polymers: These polymers were prepared in the same manner as the $\{[Cu_2(\mathbf{22})_2(dmb)_2](BF_4)_2\}_n$ and $\{[Cu_2(\mathbf{23})_2(dmb)_2](BF_4)_2\}_n$ polymers above except $[Cu_2(\mathbf{22})_2(CH_3CN)_4](BF_4)_2$ and $[Cu_2(\mathbf{22})_2(CH_3CN)_4](BF_4)_2$ were replaced by $[Ag_2(\mathbf{22})_2](BF_4)_2$ (0.100 g; 0.078 mmol) and $[Ag_2(\mathbf{23})_2](BF_4)_2$ (0.0988 g; 0.078 mmol), respectively.

$\{[Ag_2(\mathbf{22})_2(dmb)_2](BF_4)_2\}_n$: Yield 51% (66 mg), white product, m.p. 190 °C. $[\alpha]_D^{20}$ = –9.3 (*c* = 0.21, $CHCl_3$). IR (solid): $\tilde{\nu}$ = 2185, 1591, 1480, 1436, 1280, 1250 cm^{-1}. ^1H NMR (CD_3CN): δ = 7.72 (br., 2 H, Ar), 7.41 (m, 4 H, Ar), 7.15 (m, 26 H, Ar), 6.59 (br., 4 H, Ar), 3.58 (br., 4 H, CH_2), 3.44 (s, 12 H, OCH_3), 1.62–1.58 (m, 36 H, dmb) ppm. $^{13}C\{^1H\}$ NMR ($CDCl_3$): δ = 139.1 (CN), 136.9 (br., C_{arom}), 135.7 (br., C_{arom}), 133.7 (C_{arom}), 126.1 (C_{arom}), 117.8–116.9 (C_{arom}), 62.4 (C_q), 60.6 (C_q), 60.5 (O*C*H$_3$), 40.8 (*C*H), 31.9 (*C*H$_2$), 31.5 (*C*H$_2$), 31.1 (*C*H$_3$), 27.1 (P*C*H$_2$P), 26.4 (CH_3) ppm. $^{31}P\{^1H\}$ NMR ($CDCl_3$): δ = 5.1 (br. d, $^1J_{Ag-P}$ = 393 Hz) ppm. $(C_{39}H_{44}AgBF_4N_2O_2P_2)_n$: calcd. C 56.45, H 5.31, O 3.86; found C 56.34, H 5.20, O 4.14.

$\{[Ag_2(\mathbf{23})_2(dmb)_2](BF_4)_2\}_n$: Yield 82% (105 mg), white product, m.p. 154 °C. $[\alpha]_D^{20}$ = –20 (*c* = 0.48, $CHCl_3$). IR (solid): $\tilde{\nu}$ = 2174, 2134, 1599, 1586, 1435, 1372 cm^{-1}. ^1H NMR (CD_3CN): δ = 7.32 (br., 12 H, Ar), 7.17 (br., 8 H, Ar), 6.96 (br., 12 H, Ar), 3.34 (br., 4 H, CH_2), 2.12 (s, 24 H, CH_3), 1.88–1;39 (m, 36 H, dmb) ppm. $^{13}C\{^1H\}$ NMR ($CDCl_3$): δ = 143.8 (CN), 138.0–137.4 (C_{arom}), 136.1–135.2 (C_{arom}), 133.9 (C_{arom}), 48.9 (CH_3), 41.7 (C_q), 40.36 (C_q), 36.55 (*C*H), 33.3 (*C*H$_2$), 31.4 (*C*H$_2$),30.5 (*C*H$_3$), 27.4 (P*C*H$_2$P), 25.6 (*C*H$_3$) ppm. $^{31}P\{^1H\}$ NMR ($CDCl_3$): δ = 5.1 ($^1J_{Ag-P}$ = 383 Hz) ppm. $(C_{41}H_{48}AgBF_4N_2P_2)_n$: calcd. C 59.64, H 5.82; found C 59.48, H 5.63.

Thermal Gravimetric Analysis: TGA traces were acquired on a TGA 7 of Perkin–Elmer between 50 and 650 °C at 3 deg/min under nitrogen atmosphere.

Circular Dichroism Spectra: Circular dichroïsm measurements were performed on a Jasco J-810 spectropolarimeter equipped with a Jasco Peltier-type thermostat. The instrument was calibrated with an aqueous solution of (+)-10-camphorsulfonic acid at 290.5 nm. Samples were loaded into quartz cells with a path length of 0.1 cm. Far-UV CD spectra were recorded at the desired temperature from 190–700 nm by averaging three scans at 0.1 nm intervals.

X-ray Structure: Crystals were grown by slow evaporation of a CH_2Cl_2/*n*-hexanes mixture at room temperature. One single crystal of $0.10 \times 0.10 \times 0.50$ mm^3 was mounted using a glass fiber at 198(2) K on the goniometer. Data were collected on an Enraf–Nonius CAD-4 automatic diffractometer at the Université de Sherbrooke using ω scans. The DIFRAC[32] program was used for centering, indexing, and data collection. One standard reflection was measured every 100 reflections, no intensity decay was observed during data collection. The data were corrected for absorption by empirical methods based on psi scans and reduced with the NRCVAX[32] programs. They were solved using SHELXS-97[33] and refined by full-matrix least-squares on F^2 with SHELXL-97.[34] The non-hydrogen atoms were refined anisotropically. The hydrogen atoms were placed at idealized calculated geometric position and refined isotropically using a riding model. The absolute structure[35] was assigned by anomalous dispersion effects.

Acknowledgments

P. D. H. thanks the Natural Sciences and Engineering Research Council of Canada (NSERC) and Centre sur les Matériaux Optiques et Photoniques de l'Université de Sherbrooke (CEMOPUS) for fundings. Dr. Pierre Lavigne (Faculté de Médecine of the Université de Sherbrooke) is thanked for letting us use his circular dichroism spectrometer. S. J. would also like to thank Ms. M. J. Penouilh (Centre de Spectroscopie, Dijon) for help with NMR analysis and mass spectroscopy. Dr. J. Bayardon is acknowledged for the measurements of ^{11}B NMR spectra.

[1] P. D. Harvey, *Structures and Properties of Transition Metal-Containing Coordination/Organometallic Polymers and Oligomers Built Upon Assembling Diphosphine and Diisocyanide Ligands*, in: *Frontiers in Transition Metal-Containing Polymer* (Eds.: A. S. Abd-El-Aziz, I. Manners), John Wiley & Sons, New York, **2007**, pp. 321–368.
[2] P. D. Harvey, *The Spectroscopy and Photophysical Behavior of Diphosphane- and Diisocyanide-Containing Coordination and Organometallic Oligomers and Polymers: Focus on Palladium and Platinum, Copper, Silver, and Gold in Inorganic and Organometallic Macromolecules; Design and Applications* (Eds.: A. S. Abd-El-Aziz, C. E. Carraher Jr., C. U. Pittman Jr., M. Zeldin), Springer, New York, **2008**, pp. 71–107.
[3] S. J. Sherlock, M. Cowie, E. Singleton, M. M. de V. Steyn, *Organometallics* **1988**, *7*, 1663.
[4] B. Zhuang, H. Sun, G. Pan, L. He, Q. Wei, Z. Zhou, S. Peng, K. Wu, *J. Organomet. Chem.* **2001**, *640*, 127.
[5] Q.-H. Jin, L.-M. Chen, P.-Z. Li, S. F. Deng, R. Wang, *Inorg. Chim. Acta* **2009**, *362*, 5224.
[6] Q.-H. Jin, L.-M. Chen, L. Yang, P.-Z. Li, *Inorg. Chim. Acta* **2009**, *362*, 1743.
[7] C. E. Anson, L. Ponikiewski, A. Rothenberger, *Inorg. Chim. Acta* **2006**, *359*, 2263.
[8] P. Teo, L. L. Koh, T. S. A. Hor, *Inorg. Chem.* **2008**, *47*, 9561–9568.
[9] É. Fournier, A. Decken, P. D. Harvey, *Eur. J. Inorg. Chem.* **2004**, 4420.
[10] B. B. Nohra, Y. Yao, C. Lescop, R. Réau, *Angew. Chem.* **2007**, *119*, 8390; *Angew. Chem. Int. Ed.* **2007**, *46*, 8242.
[11] G. G. Lobbia, M. Pellei, C. Pettinari, C. Santini, B. W. Skelton, A. H. White, *Polyhedron* **2005**, *24*, 181.
[12] C. Di Nicola, G. A. Koutsantonis, C. Pettinari, B. W. Skelton, N. Somers, A. H. White, *Inorg. Chim. Acta* **2006**, *359*, 2159.
[13] D. Perreault, M. Drouin, A. Michel, V. M. Miskowski, W. P. Schaefer, P. D. Harvey, *Inorg. Chem.* **1992**, *31*, 695.
[14] É. Fournier, F. Lebrun, M. Drouin, A. Decken, P. D. Harvey, *Inorg. Chem.* **2004**, *43*, 3127.
[15] Y. Ouchi, Y. Morisaki, T. Ogoshi, Y. Chujo, *Chem. Asian J.* **2007**, *2*, 397.
[16] C. A. Wheaton, M. C. Jennings, R. J. Puddephatt, *Z. Naturforsch., Teil B* **2009**, *64*, 1469.
[17] C. Salomon, D. Fortin, C. Darcel, S. Jugé, P. D. Harvey, *J. Cluster Sci.* **2009**, *20*, 267.
[18] a) S. Jugé, J.-P. Genêt, J. A. Laffitte, M. Stéphan, M. Fr. Patent 91 01674 (**1991**); b) S. Jugé, R. Merdès, M. Stéphan, J.-P. Genêt, *Phosphorus Sulfur Silicon Relat. Elem.* **1993**, *77*, 199; c) C. Darcel, J. Uziel, S. Jugé, in: *Phosphorus Ligands in Asymmetric Catalysis Synthesis and Applications* (Ed.: A. Börner), Wiley-VCH, **2008**, *3*, p. 1211; d) C. C. Bauduin, D. Moulin, E. B. Kaloun, C. Darcel, S. Jugé, *J. Org. Chem.* **2003**, *11*, 4293–4301.
[19] a) J. Diez, M. P. Gamasa, J. Gimeno, A. Tiripicchio, M. Tiripicchio Camellini, *J. Chem. Soc., Dalton Trans.* **1987**, 1275; b) B. Ahrens, P. G. Jones, *Acta Crystallogr., Sect. C* **1998**, *54*, 16.
[20] P. D. Harvey, *Coord. Chem. Rev.* **1996**, *153*, 175.
[21] D. Perreault, M. Drouin, A. Michel, P. D. Harvey, *Inorg. Chem.* **1993**, *32*, 1903.
[22] A. F. M. J. Van der Ploeg, G. van Koten, *Inorg. Chim. Acta* **1981**, *51*, 225–239.
[23] D. Fortin, M. Drouin, M. Turcotte, P. D. Harvey, *J. Am. Chem. Soc.* **1997**, *119*, 531.
[24] P. D. Harvey, M. Drouin, T. Zhang, *Inorg. Chem.* **1997**, *36*, 4998.
[25] M. Turcotte, P. D. Harvey, *Inorg. Chem.* **2002**, *41*, 1739.
[26] D. Fortin, M. Drouin, P. D. Harvey, *J. Am. Chem. Soc.* **1998**, *120*, 5351.
[27] S. Sicard, J.-F. Bérubé, D. Samar, A. Massaoudi, F. Lebrun, J.-F. Fortin, D. Fortin, P. D. Harvey, *Inorg. Chem.* **2004**, *43*, 5321.
[28] É. Fournier, S. Sicard, A. Decken, P. D. Harvey, *Inorg. Chem.* **2004**, *43*, 1491.
[29] J.-F. Bérubé, K. Gagnon, D. Fortin, A. Decken, P. D. Harvey, *Inorg. Chem.* **2006**, *45*, 2812.
[30] W. P. Weber, G. W. Gokel, I. K. Ugi, *Angew. Chem.* **1972**, *84*, 587; *Angew. Chem. Int. Ed. Engl.* **1972**, *11*, 530.
[31] C. Salomon, S. Dal Molin, D. Fortin, Y. Mugnier, R. T. Boeré, S. Jugé, P. D. Harvey, *Dalton Trans.* **2010**, *39*, 10068.
[32] H. D. Flack, E. Blanc, D. Schwarzenbach, *J. Appl. Crystallogr.* **1992**, *25*, 455.
[33] E. J. Gabe, Y. Le Page, J.-P. Charland, F. L. Lee, P. S. White, *J. Appl. Crystallogr.* **1989**, *22*, 384.
[34] G. M. Sheldrick, *SHELXS-97*, G. M. Sheldrick, University of Göttingen, Germany, **1997**, rel. 97-2.
[35] H. D. Flack, *Acta Crystallogr., Sect. A* **1983**, *39*, 876.

Received: February 16, 2011
Published Online: April 7, 2011

